Classification
Physics Abstracts
61.30G — 42.65 — 64.70M

Multistability and non linear dynamics of the optical Fréedericksz transition in homeotropically aligned nematics

G. Abbate, P. Maddalena, L. Marrucci, L. Saetta and E. Santamato

Dipartimento di Scienze Fisiche, Pad. 20, Mostra d'oltremare, 80125 Napoli, Italy

(*Received 28 November 1990, accepted 7 February 1991*)

Résumé. — On présente un modèle simple et nouveau pour décrire la dynamique de la réorientation optique obtenue par un rayon laser dans un cristal liquide nématique aligné homéotropiquement. Contrairement aux précédents modèles sur ce sujet, on a rendu compte de l'échange du moment angulaire entre la lumière et le milieu. On a trouvé une dynamique riche et assez inattendue, même dans le cas d'une polarisation linéaire de la lumière incidente.

Abstract. — A new simple model is presented to describe the dynamics of the optical reorientation induced by a laser beam into a homeotropically aligned nematic liquid crystal. Unlike previous models on the subject, we accounted for transfer of angular momentum from light to the sample. A rich and somewhat unexpected dynamics is found also in the case of linear polarization of the incident light.

1. Introduction.

The Optical Fréedericksz Transition (OFT) was first observed in Nematic Liquid Crystals (NLC) by using a linearly polarized laser beam at normal incidence [1]. The effect consists in a strong optically induced reorientation of the mean direction **n** of the molecules in the sample, when the laser intensity exceeds a characteristic threshold. The unit vector **n** is called the molecular director.

It is commonly accepted that this effect is very similar to the well known Fréedericksz transition induced in nematics by external static fields [2]. It is argued, in fact, that, in view of the linear polarization of the light inside the sample, the liquid crystal molecules feel an average optical field which is constant both in intensity and in direction. Consequently, all models proposed in the literature to explain the phenomenon retain this picture and lead to results that are very similar to the ones obtained in the static-field case [3].

Nevertheless, some recent experiments [4] have shown that the interaction between nematics and light is essentially different from the interaction between nematics and static fields because liquid crystals directly couple with the *angular momentum* carried by the optical field. In simple geometries, the transfer of angular momentum from the radiation to the liquid crystal may lead to Self-Induced Stimulated Light Scattering [5].

This suggests that also in the simplest case, namely in the optical Fréedericksz transition with linearly polarized light at normal incidence, the coupling between the angular momentum of the light and the LC medium cannot be ignored so that completely new features should appear having no analog in the static-field case.

In this work a simple model is presented for the OFT with linearly polarized light at normal incidence where angular momentum balance is taken into account. It will be shown that unforeseen effects as multistability, hysteresis and oscillating relaxation toward steady-state appear naturally as a consequence of angular momentum transfer. All these effects, that may occur also very near to the threshold for the OFT, cannot be derived from the known models and their observation was never reported in the literature, although they should be certainly observable in accurate measurements.

The main difference between our model and all others reported in the literature is that we allow for a precessional motion of the director **n** around the direction of propagation of the laser beam even if the laser beam is linearly polarized. In all previous works, in fact, **n** was bound to stay in the plane formed by the polarization direction and the propagation direction of the beam. Releasing these constraints leads to the occurrence of new phenomena, related to angular momentum transfer, that will be the main object of study of this work.

Since our theoretical model seems to be interesting in its own right and differs sensibly from all other models existing in the literature, it will be the object of the present paper. The experiments about the observation of the new effects expected from the model will be presented in separate paper.

This work is organized as follows : in section 2 the relevant geometry is presented and the general equations governing the motion of the molecular director as well as the change in the polarization of the laser beam are derived from a general Lagrangian formalism, presented elsewhere [6].

In section 3 the equations are specialized to the case under study and some approximations are used to put them in a simpler form. The validity of the approximations involved is also discussed.

Finally, in section 4 the new effects expected on the basis of the model are presented and their eventual experimental observation is discussed.

2. The model.

The results presented in this section have been already reported in [6].

We consider a thin film of NLC of thickness L between glass plane walls coated with surfactant for homeotropic alignment. The anchoring at the wall is supposed to be strong. The local alignment of the molecules in the film is accounted for by the unit vector $\mathbf{n}(\mathbf{r})$. Due to the homeotropic anchoring, in the absence of external field **n** is uniformly directed along the z-axis normal to the sample walls. At some instant a monochromatic laser beam with an arbitrary polarization is focused at normal incidence onto the film. When the intensity I of the beam at the sample reaches the characteristic threshold I_{th} for the OFT, the molecular director is reoriented and changes in time until a final steady state is reached. As shown by the experiment reported in [4], the final steady state may also be time dependent, corresponding to a continuous precession of **n** around the z-axis. In the case of linear polarization of the incident beam, however, both experiment and theory lead to a time independent final state.

The basic equations governing the interaction between the director **n** and the laser optical field have been derived in [6] in the limit of plane wave (all fields depend on z only) and of slow envelope. Both these approximations are largely exploited in the literature and usually met in ordinary experiments. In particular, the consistency of the slow envelope approximation (often referred to as the Geometric Optics Approximation (GOA)) requires that the material birefringence is low, viz. $\Delta n = n_e - n_o \ll 1$, where n_e and n_o are the extraordinary and ordinary indexes of the material. This condition is usually satisfied in ordinary nematic liquid crystals. Moreover, light absorption is neglected, so that the only effect of the sample on the laser beam is a change of its polarization.

In the following, the director **n** will be described by means of its polar and azimuthal angles ϑ and ϕ [$\mathbf{n} = (\sin \vartheta \cos \phi, \ \sin \vartheta \sin \phi, \cos \vartheta)$]. Because nematics are not polar, **n** and $-\mathbf{n}$ are physically indiscernible, so that we have one-to-one correspondence with distinct physical states by taking ϑ in the range $[0, 1/2\ \pi]$ and ϕ in the range $[-\pi, \pi]$.

The polarization of the laser beam may be described by means of its ellipticity e and ellipse orientation angle ψ. (The absolute value of e is the ratio between the minor and major axis of the beam polarization ellipse and its sign is positive for left-handed polarization and negative for right-handed polarization. The angle ψ is the angle formed by the ellipse major axis with respect to an x-axis fixed in the laboratory.) It turns out to be useful introducing also the quantity $\ell_z = -(I/\omega)\, e$, where $\omega = 2\pi/\lambda$ is the frequency of the laser beam and I its intensity (average Poynting vector along z). It is evident that ℓ_z is the component of the average angular momentum carried by the beam along its propagation direction.

The time-independent equation of motion for the azimuthal angle ϕ and the polar angle ϑ of the director can be obtained from the minimization of the total (elastic + optical) free-energy [6]

$$F = F_0 + W, \tag{1}$$

where F_0 is the elastic free energy density of the NLC, given by

$$\begin{aligned} F_0 = & \frac{1}{2}(k_{22}\sin^2\vartheta + k_{33}\cos^2\vartheta)\sin^2\vartheta\,(\mathrm{d}\phi/\mathrm{d}z)^2 + \\ & + \frac{1}{2}(k_{11}\sin^2\vartheta + k_{33}\cos^2\vartheta)\,(\mathrm{d}\vartheta/\mathrm{d}z)^2 \end{aligned} \tag{2}$$

and W is the energy density of the optical field, that can be written out in terms of e and ψ as

$$W = (In_o/c) + (I/2\,c)\,\Delta n(\vartheta)\left\{1 + \sqrt{1-e^2}\cos\left[2(\psi - \phi)\right]\right\}. \tag{3}$$

In equations (2) and (3) k_{ii} denote the NLC elastic constants and c the speed of light (cgs units are used). Finally, the birefringence $\Delta n(\vartheta)$ as seen by the optical wave is given by

$$\Delta n(\vartheta) = \frac{n_e\, n_o}{\sqrt{n_e^2\cos^2\vartheta + n_o^2\sin^2\vartheta}} - n_o. \tag{4}$$

As stressed in [6], the total free-energy F must be considered as a Hamiltonian H for the whole system, provided we introduce the quantities

$$\begin{aligned} p_\phi &= (k_{22}\sin^2\vartheta + k_{33}\cos^2\vartheta)\sin^2\vartheta\,(\mathrm{d}\phi/\mathrm{d}z) \\ p_\vartheta &= (k_{11}\sin^2\vartheta + k_{33}\cos^2\vartheta)(\mathrm{d}\vartheta/\mathrm{d}z) \\ p_\psi &= -\ell_z = +(I/\omega)\, e \end{aligned} \tag{5}$$

as moments conjugate to the generalized coordinates ϕ, ϑ and ψ, respectively, and express F as $F = H(\phi, \vartheta, \psi, p_\phi, p_\vartheta, p_\psi)$.

Immediate consequences of this Hamiltonian formulation is that, in time-independent states, H itself (i.e. the total free-energy F) is constant along the sample ($F =$ const.) and so is the quantity

$$p_\psi + p_\phi = (k_{22}\sin^2\vartheta + k_{33}\cos^2\vartheta)\sin^2\vartheta\,(\mathrm{d}\phi/\mathrm{d}z) + (I/\omega)\,e = \text{const.} \tag{6}$$

The conservation law (6) expresses the conservation of the total (elastic plus optical) average angular momentum flux along the beam propagation direction.

The distortion angles $\phi(z)$ and $\vartheta(z)$ as well as the polarization state $\psi(z)$, $e(z)$ along the sample are obtained from Hamilton's equations :

$$\mathrm{d}\phi/\mathrm{d}z = \frac{p_\phi}{(k_{22}\sin^2\vartheta + k_{33}\cos^2\vartheta)\sin^2\vartheta} \tag{7a}$$

$$\mathrm{d}\vartheta/\mathrm{d}z = \frac{p_\vartheta}{k_{11}\sin^2\vartheta + k_{33}\cos^2\vartheta} \tag{7b}$$

$$\mathrm{d}p_\phi/\mathrm{d}z = -(I/c)\,\Delta n(\vartheta)\sqrt{1-e^2}\sin[2(\psi-\phi)] \tag{7c}$$

$$\mathrm{d}p_\vartheta/\mathrm{d}z = -(I/2c)\,\Delta n'(\vartheta)\left\{1+\sqrt{1-e^2}\cos[2(\psi-\phi)]\right\} + \\ + \sin\vartheta\cos\vartheta\left\{(k_{33}-k_{11})(\mathrm{d}\vartheta/\mathrm{d}z)^2 - [k_{33}-2(k_{33}-k_{22})\,.\sin^2\vartheta]\,(\mathrm{d}\phi/\mathrm{d}z)^2\right\} \tag{7d}$$

$$\mathrm{d}\psi/\mathrm{d}z = -(\omega/2c)\,\Delta n(\vartheta)\left(\frac{e}{\sqrt{1-e^2}}\right)\cos[2(\psi-\phi)] \tag{7e}$$

$$\mathrm{d}e/\mathrm{d}z = (\omega/c)\,\Delta n(\vartheta)\sqrt{1-e^2}\sin[2(\psi-\phi)]\,. \tag{7f}$$

Equations (7a-f) must be supplemented with boundary conditions at the sample walls. For homeotropic alignment these are

$$\vartheta(0) = \vartheta(L) = 0\,; \qquad \mathrm{d}\phi/\mathrm{d}z\,(0) = \mathrm{d}\phi/\mathrm{d}z(L) = 0\,. \tag{8}$$

Moreover, we must impose $e(0) = e_0$ and $\psi(0) = \psi_0$ at the input plane $z = 0$, where e_0 and ψ_0 are the ellipticity and ellipse angle of the incident laser beam.

These results hold for time-independent states only. In the not stationary case we must add phenomenological viscous terms on the left of equations (7c) and (7d) having the form $-\gamma\sin^2\vartheta\,\partial\phi/\partial t$ and $-\gamma\,\partial\vartheta/\partial t$, respectively, where γ is an appropriate viscosity coefficient, and change all total derivatives into partial derivatives ($\mathrm{d}/\mathrm{d}z \to \partial/\partial z$) [7]. In this case, the angular momentum balance equation assumes the form

$$\gamma\int_0^L \partial\phi/\partial t\,\sin^2\vartheta\,\mathrm{d}z = (I/\omega)\,\Delta e\,, \tag{9}$$

where $\Delta e = e(L) - e(0)$ is the change of the polarization ellipticity suffered by the beam in traversing the sample.

Finally, we note that equations (7e) and (7f) can be rewritten in terms of Stokes' reduced parameters s_i ($i = 1, 2, 3$) in the simpler form

$$\mathrm{d}\mathbf{s}/\mathrm{d}z = \mathbf{\Omega}_1 \times \mathbf{s} \tag{10}$$

where $\mathbf{s} = (s_1, s_2, s_3)$ with

$$s_1 = \sqrt{1-e^2}\cos 2\psi \\ s_2 = \sqrt{1-e^2}\sin 2\psi \\ s_3 = e \tag{11}$$

and $\mathbf{\Omega} = \mathbf{\Omega}_1(\vartheta, \phi)$ is given by

$$\mathbf{\Omega}_1 = (\omega/c)\, \Delta n(\vartheta)\, (\cos(2\phi), \sin(2\phi), 0) . \tag{12}$$

The boundary conditions on equation (12) are evidently $\mathbf{s}(0) = (s_{10}, s_{20}, s_{30})$, where s_{10}, s_{20} and s_{30} are the Stokes parameters of the incident beam.

3. The simplified model.

Equations (7a-f) describe the laser induced molecular reorientation in the NLC and the change in polarization of the beam in the plane-wave and slow envelope approximations. It is evident that these equations are very awkward, so we need simplification.

In view of the boundary conditions (8), which must hold at any time t, we may expand $\vartheta(z, t)$ as

$$\vartheta(z, t) = \sum_{n=0}^{\infty} \vartheta_n(t) \sin(n\pi z/L) . \tag{13}$$

For laser intensity very close to the threshold to induce the OFT, ϑ is small and we may retain only the first term in the sum (13), so that

$$\vartheta(z, t) \simeq \vartheta_1(t) \sin(\pi z/L) . \tag{14}$$

Moreover, since ϑ is small, we retain only terms up to ϑ^3 in equations (7b) and (7c). This yields the following approximate equation for ϑ :

$$\frac{\partial \vartheta}{\partial t} = (1 - k\vartheta^2) \frac{\partial^2 \vartheta}{\partial z^2} - k\vartheta \frac{\partial \vartheta}{\partial z} + \pi^2 \tilde{I} \left(\vartheta - \frac{4}{3} A \vartheta^3 \right) (1 + s_{10} \cos 2\phi) , \tag{15}$$

where we posed

$$\begin{aligned} \tau &= \left(\frac{k_{33}}{\gamma_1 L^2} \right) t \\ k &= 1 - \frac{k_{11}}{k_{33}} \\ \delta &= \frac{n_e}{n_o} \\ A &= \frac{9 - 5\delta^2}{8\delta^2} \\ \tilde{I} &= \frac{I}{I_{th}} \\ I_{th} &= \frac{c\pi^2 \delta^2 k_{33}}{n_o L^2(\delta^2 - 1)} . \end{aligned} \tag{16}$$

I_{th} is the threshold intensity for the OFT with linearly polarized light. The same expression of I_{th} was obtained with a different approach in [2].

Experiments show that the azimuthal ϕ angle may rotate over several π, so we cannot consider it small in general. Nevertheless we assume that, in view of the boundary conditions (8), which are « free » for ϕ, we may neglect the *twist* of ϕ in the interior of the cell. In other words, we assume $\phi(z, t)$ large, but $\partial\phi/\partial z$ small ($\partial\phi/\partial z$ is exactly zero at the walls). At the zero-order approximation we have $\partial\phi/\partial z \equiv 0$, so that $\phi = \phi(t)$ only. Inserting then equation (14) into equation (15), multiplying by $\sin(\pi z/L)$ and integrating from $z = 0$ to $z = L$ yields a single equation for $\vartheta_1(\tau)$:

$$\dot{\vartheta}_1(\tau) = -\pi^2\vartheta_1\left(1 - \frac{1}{2}k\vartheta_1^2\right) + \frac{1}{2}\pi^2\tilde{I}\vartheta_1(1 - A\vartheta_1^2)(1 + s_{10}\cos 2\phi), \qquad (17)$$

where $\dot{\vartheta}_1 = d\vartheta_1/d\tau$ and the reduced time τ is given by the first of equations (16).

The evolution equation for $\phi(\tau)$ is obtained directly from the angular momentum balance equation (9). Inserting expression (14) for $\vartheta(z, \tau) \ll 1$ and assuming ϕ independent of z, the integration in equation (9) can be performed yielding

$$\dot{\phi}(\tau) = \frac{\pi^2\delta^2\tilde{I}}{2(1+\delta)\tilde{L}}[s_3(\tilde{L}, \tau) - s_{30}], \qquad (18)$$

where we introduced the dimensionless thickness $\tilde{L} = (\omega/c)n_0(\delta - 1)L$.

Within these approximations, the equation (10) governing the change of the beam polarization can be solved analytically. It is convenient passing to the new independent variable $u(z, \tau)$ defined by $\partial u/\partial z = (\omega/c)\Delta n(\vartheta(z, \tau))$. Then we obtain $\partial\mathbf{s}/\partial u = \tilde{\mathbf{\Omega}}_1(\tau) \times \mathbf{s}$, with $\tilde{\mathbf{\Omega}}_1(\tau) = (\cos 2\phi(\tau), \sin 2\phi(\tau), 0)$, whose solution is

$$\mathbf{s}(u(z, \tau)) = \tilde{\mathbf{\Omega}}_1(\tilde{\mathbf{\Omega}}_1 \cdot \mathbf{s}_0) + [(\tilde{\mathbf{\Omega}}_1 \times \mathbf{s}_0) \times \tilde{\mathbf{\Omega}}_1]\cos(u) + (\tilde{\mathbf{\Omega}}_1 \times \mathbf{s}_0)\sin(u). \qquad (19)$$

Moreover, using equations (4) and (14) and since $\vartheta \ll 1$, we find

$$\begin{aligned} u(z, \tau) &= (\omega/c)\int_0^L \Delta n(\vartheta(z, \tau))\,dz \\ &= \alpha(\tau)[(z/L) - (1/2\pi)\sin(2\pi z/L)], \end{aligned} \qquad (20)$$

where we introduced the birefringence phase angle $\alpha(\tau)$ given by

$$\alpha(\tau) = u(L, \tau) = \frac{\tilde{L}(\delta + 1)}{4\delta^2}\vartheta_1^2(\tau) = \beta\vartheta_1^2(\tau). \qquad (21)$$

The angle α is the phase difference accumulated by the optical wave in traversing the film with respect to an ordinary wave.

The polarization state $\mathbf{s}(\tau) = \mathbf{s}(\tilde{L}, \tau)$ of the light emerging from the cell is obtained from equation (19) as a function of $\phi(\tau)$ and $\vartheta_1(\tau)$, by substituting for u its end-point value $\alpha(\tau)$. In particular we may evaluate $s_3(\tilde{L}, \tau)$ and insert it into equation (18), obtaining

$$\dot{\phi}(\tau) = -\frac{1}{2}\pi^2\tilde{I}\left(s_{30}\frac{1 - \cos\alpha}{\alpha} + s_{10}\frac{\sin\alpha}{\alpha}\sin 2\phi\right). \qquad (22)$$

Finally, using again equation (21), we may rewrite equation (17) in terms of $\alpha(\tau)$:

$$\dot{\alpha}(\tau) = -\frac{1}{2}\pi^2\left\{\alpha - (k/2\beta)\alpha^2 - \frac{1}{2}\tilde{I}\alpha[1 - (A/\beta)\alpha](1 + s_{10}\cos 2\phi)\right\}. \qquad (23)$$

Equations (22) and (23) are the main result of this section. They form a set of two first-order ordinary differential equations in the unknown functions $\phi(t)$ and $\alpha(t)$. Once a solution $(\phi(\tau), \alpha(\tau))$ of equations (22) and (23) is found, the polar angle $\vartheta(z, \tau)$ is given by equation (14) and the light polarization state at each point in the sample is given by equation (19) with u derived from equation (20).

We notice that although ϑ_1 is supposed very small, we cannot consider the birefringence phase angle α as a small quantity, because the coefficient β in equation (21) may be very large in practical cases. For example, in the case of the nematic 5 CB ($n_e = 1.7$, $n_o = 1.5$) and assuming a film thickness L of 75 μm and a wavelength $\lambda = 0.515$ μm, we have $\beta = \frac{\tilde{L}(\delta + 1)}{4\delta^2} = 70$. In particular, we *cannot* expand sin α and cos α in equation (23) as a power series of α, unless $\vartheta_1 \ll \beta^{-1} \simeq 0.01$, in typical conditions.

4. The case of linear polarization.

Although equations (22) and (23) hold in general for any polarization state of the incident beam, in the following we assume the polarization to be linear, so that we have $s_{10} = 1$, $s_{20} = 0$ and $s_{30} = 0$. In this case, we see that $\alpha = 0$ and $\phi = 0$ or $\pm \pi$ are trivial steady solutions of equations (22) and (23). Obviously, $\phi = \pm \pi$ represent the same physical state. Strictly speaking, when $\alpha = 0$ the value of ϕ is undetermined. It is not so in equations (22) and (23). To understand the real physical meaning of these equations we must study their behavior in the limit of very small α. The solution of equations (22) and (23) for small α, in fact, represents the initial dynamics of the system when it is moving from the undistorted homeotropic alignment. Retaining only terms in the first order in α, equations (22) and (23) can be solved yielding

$$\phi(\tau) = \tan^{-1}(\tan \phi_0 \, e^{-2\pi^2 \tilde{I}\tau})$$

$$\alpha(\tau) = \alpha_0 \exp\left[\frac{1}{2}\pi^2(\tilde{I} - 1)\tau + \frac{1}{4}\ln\left(\frac{1 + \tan^2 \phi_0 \, e^{-2\pi^2 \tilde{I}\tau}}{1 + \tan^2 \phi_0}\right)\right], \tag{24}$$

where $\alpha_0 \ll 1$ and $-\pi \leqq \phi_0 \leqq \pi$ are the initial values of α and ϕ, respectively. If no external field except the optical field is applied to the system, the induced reorientation starts from noise and α_0 and ϕ_0 must be considered as random initial data. Notice that ϕ_0 is not bounded to be small. Equations (24) show that whenever α_0 and ϕ_0 may be, $\phi(\tau)$ tends asymptotically to 0 or $\pm \pi$ as $\tau \to \infty$, and $\alpha(\tau)$ tends asymptotically to zero for $\tilde{I} = I/I_{th} < 1$ and to infinite for $\tilde{I} = I/I_{th} > 1$. Then, in order to induce the reorientation starting from noise in the undistorted state $\alpha = 0$, we must have $\tilde{I} > 1$, i.e. I must be larger than the threshold I_{th} for the OFT. The second of equations (24) shows, however, that, for $\tilde{I} > 1$ and $\phi_0 \neq 0$, $\alpha(\tau)$ decreases first and then increases again passing through a minimum value. Only for $\phi_0 = 0$ we have an exponential grow of $\alpha(\tau)$, as claimed in all previous works. This not monotonic behavior of the birefringence α in time could be observed, for example, by preparing the system in a slightly rotated state with **n** lying in a plane forming an angle $\phi_0 \neq 0$ with the polarization of the laser beam.

As the time goes on, α increases until saturation is reached. Saturation is governed by higher-order terms in α in equation (23). An exact solution of equations (22) and (23) for linear polarization is $\phi = 0$ and $\alpha(\tau)$ given by

$$\alpha(\tau) = \frac{\alpha_0 \alpha_1}{\alpha_0 + (\alpha_1 - \alpha_0) e^{-\frac{1}{2}\pi^2(\tilde{I} - 1)\tau}}, \quad (\tilde{I} > 1) \tag{25}$$

where $\alpha_0 > 0$ is the initial value of α and

$$\alpha_1(\tilde{I}) = \frac{2\beta(\tilde{I}-1)}{2A\tilde{I}-k}. \tag{26}$$

The solution (25) was already studied in Ong's paper [8]. This solution shows that if $\alpha_1 > 0$ then $\alpha(\tau)$ tends asymptotically to the saturation value $\alpha_\infty = \alpha_1$. If $\alpha_1 < 0$, instead, $\alpha(\tau)$ grows asymptotically to infinite, so that saturation is governed eventually by terms of the order of α^4 or higher, which we have neglected in equation (23). Since $\phi \equiv 0$ along this solution, the polarization of the beam stays linear for any value of $\alpha(\tau)$.

The case $\alpha_1 < 0$ was discussed in some detail by Ong [8], who showed that, in this case, a *first order* (i.e. discontinue) OFT is to be expected. The condition $\alpha_1 < 0$ is always satisfied if the material constants are so that $k > 2A$. In view of equations (16), this is precisely the same condition obtained by Ong [8]. It is worth noting that PAA (p-azoxyanisole) and a few mixtures of nematic liquid crystals can have $k > 2A$ [9]. But, to our knowledge, any attempt made to observe a first-order OFT in these materials failed. For this reason in this work we assume α_1 positive.

We pass now to consider in some detail the steady states of the system.

a) *The steady-states.* — The steady-states of the system for linear light polarization are obtained by setting $s_{10} = 1$, $s_{30} = 0$ and $\dot{\phi} = \dot{\vartheta} = 0$ in equations (22) and (23). The resulting time-independent states $(\bar{\phi}, \bar{\vartheta})$ are given (implicitly) by

$$\sin 2\bar{\phi} \sin \bar{\alpha} = 0$$

$$\bar{\alpha} = \beta \frac{\tilde{I}(1+\cos 2\bar{\phi}) - 2}{A\tilde{I}(1+\cos 2\bar{\phi}) - k}. \tag{27}$$

Since α is positive semidefinite we must retain only solutions of equations (27) with $\bar{\alpha} \geqq 0$. Below the threshold $(\tilde{I} < 1)$, no distortion can be optically induced in the sample and the only stable state is the state $\alpha = 0$. We shall consider, therefore, only states at laser intensity $\tilde{I}$ greater than the threshold. At all steady states the polarization of the beam emerging from the sample is still linearly polarized as the input light, as required by the angular momentum conservation. If this were not the case, in fact, angular momentum would be deposited into the sample, producing rotation of the molecular director **n** around the beam axis.

A first steady state is $\bar{\phi} = 0$ (or $\pm\pi$) and $\bar{\alpha} = \alpha_1(\tilde{I})$, as given by equation (26). This is the state that the system should reach at saturation, *provided* the ϕ angle is bound to stay on the polarization plane of the incident light. As previously mentioned, this state was the only steady state considered in the literature. In this state, the polarization of the beam remains unchanged (linear) at any point in the sample. We will refer to this state as the unrotated state of the system.

Besides this state, however, we have two more sets of time-independent states, corresponding to **n** out of the light polarization plane. We will refer to these sets of states as the rotated states of the system. The two sets of states are given by $\bar{\alpha} = n\pi$ and $\bar{\phi} = \pm\bar{\phi}_n(\tilde{I})$ $(n = 0, 1, \dots)$ with n odd and n even, respectively. For each n, $\bar{\phi}_n(\tilde{I})$ is found implicitly from equation (27) as

$$\tan^2 \bar{\phi}_n = \tilde{I}\left(\frac{2\beta - 2An\pi}{2\beta - kn\pi}\right) - 1. \tag{28}$$

For the set of steady states with odd n, the optical retardation phase α is locked at π and sample behaves as a $\frac{1}{2}\lambda$-plate rotated at an angle $\bar{\phi}_n(\tilde{I})$. In these states, the polarization of the beam emerging from the sample is still linearly polarized, but is rotated with respect to the incident polarization direction of an angle $2\,\bar{\phi}_n(\tilde{I})$, depending on the incident power. This fixed-retardation behavior may be useful for applications. A standard Lyapounov's stability analysis shows that these states are stables foci (unless $\bar{\phi}_n$ is very small, in which case they are stable nodes). It is expected, therefore, that the director **n** approaches these states with damped oscillations.

In the set of steady states with even n, the sample behaves as a λ-plate. In these states, the beam emerges with the same polarization as it enters, although the polarization state may vary inside the film. These states are found to be unstable saddle points and should be not observed.

A plot of $\phi_n(\tilde{I})$ for both sets of states is shown in figure 1, the dashed curves referring to the unstable states.

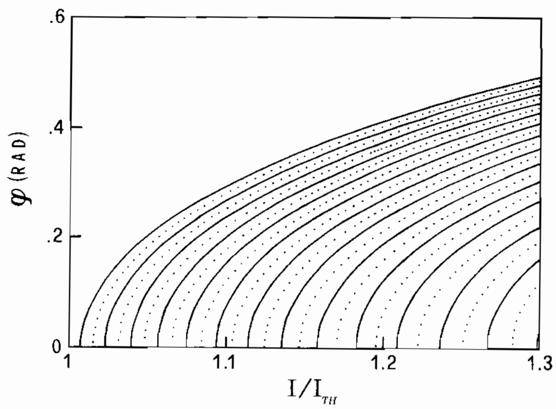

Fig. 1. — Steady-state director ϕ-angle as a function of intensity $\tilde{I}$, Solid curves refer to $\alpha = n\pi$ with odd n and are stable states. Dashed refer to $\alpha = n\pi$ with even n and are unstable states. In the numerical calculations we used typical values for nematic 5 CB as reported in Ong's paper [3] and film thickness $L = 75\ \mu m$ and wavelength $\lambda = 0.514\ \mu m$.

The rotated states coalesce with the unrotated state $\phi = 0$, $\alpha = \alpha_1(\tilde{I})$ at characteristic branching points $\tilde{I} = \tilde{I}_n$ $(n = 0, 1, \ldots)$ given by $\alpha_1(\tilde{I}_n) = n\pi$, viz.

$$\tilde{I}_n = \frac{2\,\beta - kn\pi}{2\,\beta - 2\,An\pi} \cong 1 + \frac{n\pi}{\beta}\,(2\,A - k) \quad (n = 0, 1, \ldots)\,. \tag{29}$$

In the last term we used the fact that β is large. We notice that because in all practical cases β is large and A and k are of the same order of magnitude, the difference $\Delta\tilde{I} = \tilde{I}_{n+1} - \tilde{I}_n$ is usually very small, i.e. the branching points on the curve $\bar{\alpha}(\tilde{I})$ are very dense. In accordance with the alternating stability of the rotated states, it turns out that the unrotated state changes its stability at the branching points (29). Unlike claimed in all previous work, the present analysis shows, therefore, that the unrotated state is sometime destabilized by the ϕ degree of freedom. This is made evident by linearizing equations (22) and (23) around the unrotated state $\phi = 0$, $\alpha = \alpha_1(\tilde{I})$. The fluctuations $\delta\alpha$ and $\delta\phi$ around this state are found to be

$$\delta\alpha(\tau) \to \delta\alpha_0 \exp\left[-\frac{1}{2}\pi^2(\tilde{I}-1)\tau\right] \to 0$$
$$\delta\phi(\tau) \to \delta\phi_0 \exp\left[-(\pi^2\tilde{I})\frac{\sin\alpha_1}{\alpha_1}\tau\right] \to \begin{cases} 0 & \text{for } \sin\alpha_1 > 0 \\ \infty & \text{for } \sin\alpha_1 < 0 . \end{cases} \tag{30}$$

We see that the fluctuations of the angle α (or ϑ) are damped out, but the fluctuations of the ϕ angle may grow in time if $\sin\alpha_1 < 0$. The motion of the director **n** is henceforth asymptotically stable if $\sin\alpha_1 > 0$ and asymptotically unstable if $\sin\alpha_1 < 0$. Therefore, if the laser intensity $\tilde{I}$ is so that

$$\tilde{I}_n < \tilde{I} < \tilde{I}_{n+1} \quad \text{with odd } n , \tag{31}$$

the molecular director will deviate out of the plane of polarization of the light (plane $\phi = 0$) and will reach finally some equilibrium state which is rotated at an angle $\phi \neq 0$. The saturated undistorted state $\phi = 0$, $\alpha = \alpha_1(\tilde{I})$ is unstable and cannot be reached by the system.

It should be pointed out, however, that even in the cases where the unrotated state $\phi = 0$ is stable, it may happen that the *dynamics* of the system may drive it to some other rotated ($\phi \neq 0$) stable state, preventing it from reaching the state $\phi = 0$, $\alpha = \alpha_1(\tilde{I})$.

b) *The dynamics.* — The system is characterized by a large number of steady states, so its dynamics is complex. The differential equations (22) and (23) have been numerically integrated for the case of linear polarization. The results are reported in figure 2, where the

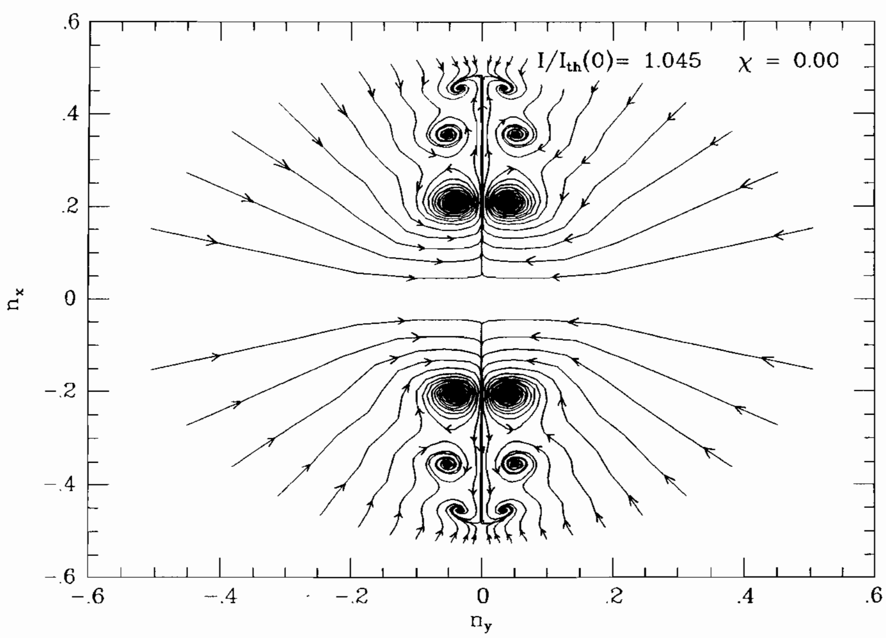

Fig. 2. — Trajectories of the director **n** in the (n_x, n_y)-plane for linear polarization and $\tilde{I} = 1.045$. For this intensity no stable state exists at $\phi = 0$.

trajectories followed by the director **n** in the xy-plane are drawn. The figure refers to a case where $\tilde{I}$ is in the interval (31), so that no stable state exists with $\phi = 0$. The figure shows that if the initial state is close enough to the undistorted state $\alpha = 0$, the system will evolve towards a rotated final state, executing damped oscillations in both $n_x = \sin \vartheta \cos \phi$ and $n_y = \sin \vartheta \sin \phi$. This oscillating approach to equilibrium should be experimentally observable. Similar results are obtained in the case where $\tilde{I}$ is not in the interval (31). The unrotated state can now be reached, since it is stable, but many trajectories still exist that fall spiraling around some other rotated state.

Moreover we found that the dynamics of **n** is very sensitive to the ellipticity parameter $\chi = \frac{1}{2} \sin^{-1}(s_{30})$ of the input beam. A value of χ as small as 0.01, for example, drives the director to a quite different final steady-state, as it is shown in figure 3. We notice that the symmetry in the change $\phi \rightarrow -\phi$ is strongly broken for $\chi \neq 0$, so that, for instance, the state C which is the symmetric of the stable state B, becomes actually unstable.

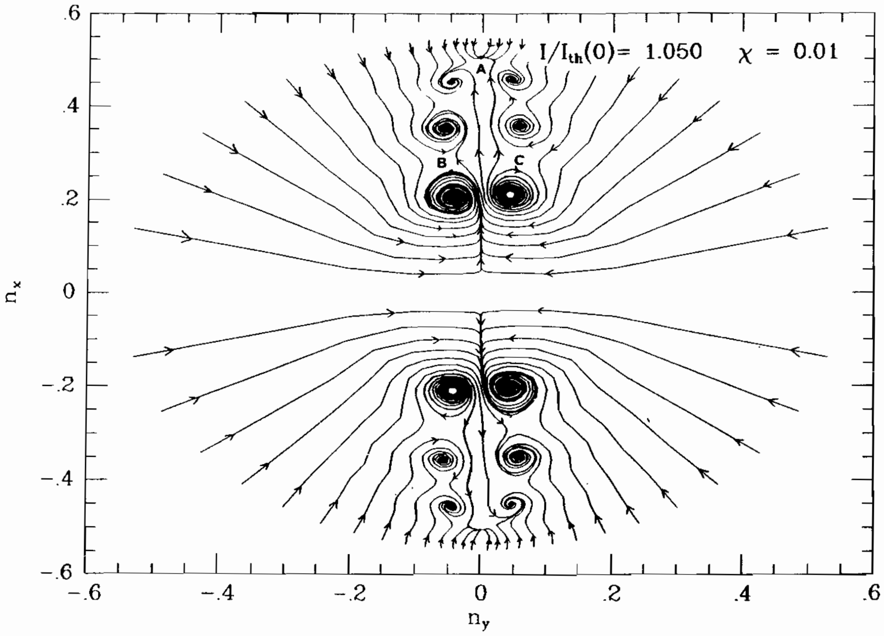

Fig. 3. — Trajectories of the director **n** in the (n_x, n_y)-plane for almost linear polarization ($\chi = 0.01$) and $\tilde{I} = 1.05$. Trajectories starting from small α end onto the state B instead of A, as it happens for exactly linear polarization. Unlike state B, the state C is unstable.

5. The case of circular polarization.

Putting $s_{10} = 0$, $s_{30} = \pm 1$ in equations (22) and (23) they can be solved in the form

$$\alpha(\tau) = \frac{\alpha_0 \alpha_2}{\alpha_0 + (\alpha_2 - \alpha_0) e^{-\frac{1}{4}\pi^2(\tilde{I} - 2)\tau}} \rightarrow \alpha_2 \quad \text{as} \quad \tau \rightarrow \infty$$

$$\phi(\tau) = \phi_0 - (\pi^2 \tilde{I}) \int_0^\tau \frac{\sin^2 \frac{1}{2} \alpha(s)}{\alpha(s)} ds \rightarrow \phi_0 + \tilde{\Omega} \tau \quad \text{as} \quad \tau \rightarrow \infty, \tag{32}$$

with

$$\tilde{\Omega} = -(\pi^2 \tilde{I}) \frac{\sin^2 \frac{1}{2} \alpha_2}{\alpha_2}$$

$$\alpha_2 = \frac{\beta(\tilde{I}-2)}{A\tilde{I}-k} . \tag{33}$$

Wee see that, provided $\tilde{I} > 2$ (which is the threshold to induce reorientation with circularly polarized light) after a transient the system is put into uniform rotation with constant asymptotic angular velocity $\tilde{\Omega}$ [10]. The asymptotic motion of **n** is actually a uniform precession around the beam propagation direction with fixed tilt angle $\vartheta_2 = \sqrt{\alpha_2/\beta}$ and angular velocity $\tilde{\Omega}$. This precessional motion was effectively observed in [3]. A plot of $\tilde{\Omega}$ and ϑ_2 as functions of the reduced intensity $\tilde{I}$ is shown in figure 4. The zeroes of $\tilde{\Omega}$ correspond to the vanishing of the angular momentum transfer [see Eq. (18)].

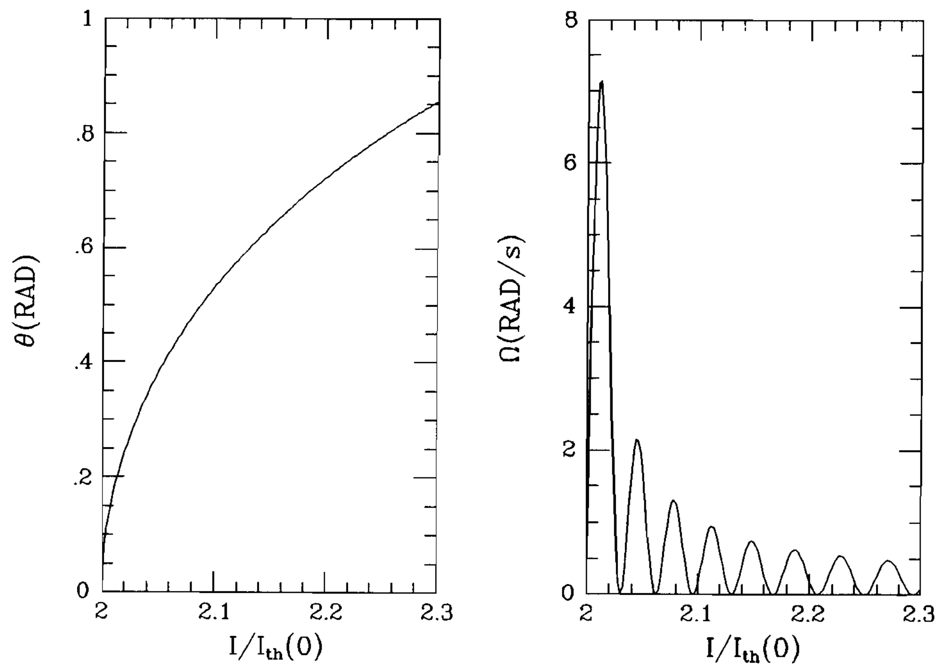

Fig. 4. — Polar angle ϑ and angular velocity Ω as functions of $\tilde{I}$ for circular polarization of the input beam.

The stability analysis of the solution (32) is made in the usual way by considering small fluctuations $\delta\phi(\tau)$ and $\delta\alpha(\tau)$. We find

$$\delta\alpha(\tau) = \delta\alpha_0 \, e^{-\frac{1}{4}\pi^2(\tilde{I}-2)\tau}$$

$$\delta\dot{\phi}(\tau) = \delta\tilde{\Omega}(\tau) = \pi^2\left(\frac{1-\cos\alpha_2-\alpha_2\sin\alpha_2}{2\alpha_2}\right)\delta\alpha_0 \, e^{-\frac{1}{4}\pi^2(\tilde{I}-2)\tau} . \tag{34}$$

Both the fluctuations of the angle α (or ϑ) and of the angular velocity $\tilde{\Omega}$ tend to be damped out in time above the threshold, so the precession motion is orbitally stable. We notice however, that the hysteretic behavior of this regime as reported in [3] is not found in the limit of the present model. This may be due to some amount of twist inside the sample which tends to overstabilize the precession motion, leading to hysteresis. A generalization of the present model accounting also for twist should be then advisable, in order to explain the experimental observations.

6. The case of elliptical polarization.

In the case of elliptical polarization, the director dynamics can be studied solving equations (22) and (23) numerically. Typical results are shown in figures 5 and 6.

The threshold to induce reorientation for general χ is given by

$$\tilde{I}_{\text{th}}(\chi) = \frac{2}{1+\cos 2\chi} . \tag{35}$$

For $\tilde{I} > \tilde{I}_{\text{th}}(\chi)$, two possible asymptotic regimes were found :

1) Stationary steady states.
2) Limit cycles.

Limit cycles, however, have never been found for $\chi < \bar{\chi} \simeq 0.4$.

As shown in figures 4 and 5, for $\chi > \bar{\chi}$, the limit cycle is reached when the laser intensity $\tilde{I}$ is increased to destabilize the two foci at the center of the figures. The limit cycle corresponds actually to a non-uniform precession-nutation of **n** around the laser beam axis. The observation of this kind of regimes was actually reported in [4]. The persistent oscillation regimes observed in the second of [4] was not found, however, from our model. As we pointed out at the end of section 5 for the hysteresis of the rotation regime, the occurrence of persistent oscillations could be essentially related to the presence of twist in the sample, which is completely neglected in the present model.

7. Final remarks.

Although the model presented in this paper is in many respects oversimplified, it shows clearly that the transfer of angular momentum from a light beam to a liquid crystalline medium leads, in general, to peculiar dynamical effects having no analog in the d.c.-field case. Some of these effects have been observed experimentally using circular or elliptical polarization [4]. In all reported experiments on the Optical Fréedericksz Transition with linear polarization at normal incidence, instead, neither multistability was found nor oscillating relaxation to equilibrium was reported [1]. We believe that this is due to the fact that in usual experiments the phase retardation α was measured by simply looking at the diffraction rings in the far field pattern beyond the sample (yielding to an accuracy on α of roughly $\pm\pi$) and that the power of the incident beam was varied in relatively large steps. In

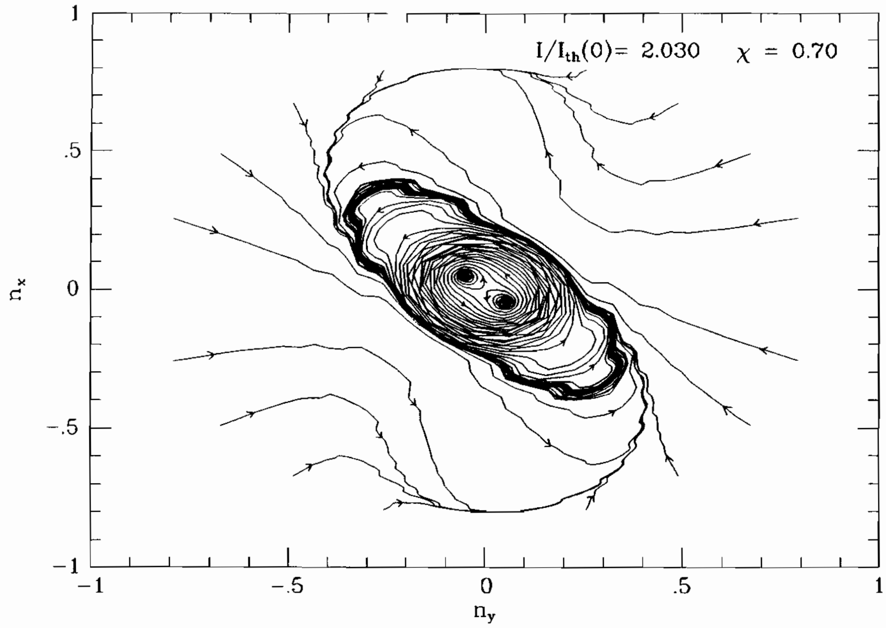

Fig. 5. — Trajectories of the director **n** in the (n_x, n_y)-plane for elliptical polarization ($\chi = 0.7$) and $\tilde{I} = 1.9$. All trajectories end in a stable state.

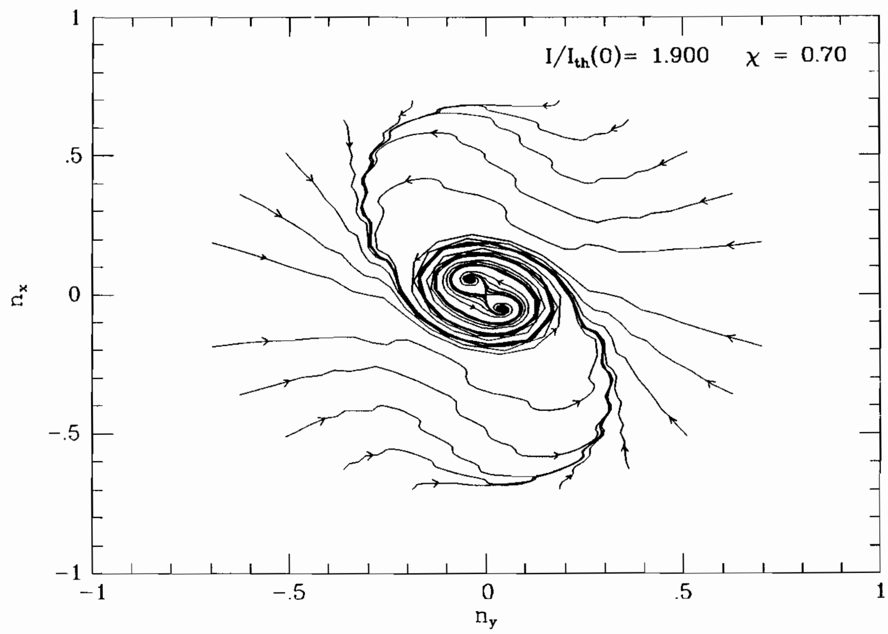

Fig. 6. — Trajectories of the director **n** in the (n_x, n_y)-plane for elliptical polarization ($\chi = 0.7$) and $\tilde{I} = 2.03$. All trajectories end in a limit cycle.

order to resolve the multistable structure shown in figure 1, in fact, the incident power should be varied in very small amounts, of the order of 1 % each, and the phase retardation α should be measured with much better accuracy. The *dynamics* of the system, in fact, is so that if the angle ϕ is initially small and the intensity I is suddenly increased in steps much larger than the difference $\Delta \tilde{I}$ between two successive thresholds $\tilde{I}_n$ for instability (Eq. (27)), ϕ can never become large and, approximately, the steady-state value of α is always very close to the value given by equation (26), according to the experimental observations made in [1]. Large values of ϕ and the locking of α at half integer π could be observed only by driving the system adiabatically along one of the stable branches in figure 1, which requires very accurate control of the laser power. In view of the high long term stability of c.w. laser available today, however, the observation of the multistability and the locking of the phase α in the OFT should be not beyond the actual experimental possibility [11].

Acknowledgments.

This work was supported by Ministero della Università e della Ricerca Scientifica e Tecnologica and by Consiglio Nazionale delle Ricerche, Italy.

References

[1] DURBIN D., ARAKELIAN S. M. and SHEN Y. R., *Phys. Rev. Lett.* **47** (1981) 1411.

[2] For a discussion on the Fréedericksz transition induced by static fields see, for example, SAUPE A., *Z. Naturforsch.* **A 15** (1960) 815.

[3] ZEL'DOVICH B. Ya and TABIRYAN N. V., *Zh. Exp. Teor. Fiz.* **81** (1981) 72 [*Sov. Phys. JEPT* **54** (1981) 32]. For a more extensive review on the OFT see also ONG H. L., *Phys. Rev.* **A 28** (1983) 2393 and references therein.

[4] SANTAMATO E., DAINO B., ROMAGNOLI M., SETTEMBRE M., SHEN Y. R., *Phys. Rev. Lett.* **57** (1986) 2423 ;
SANTAMATO E., ABBATE G., MADDALENA P., MARRUCCI L., SHEN Y. R., *Phys. Rev. Lett.* **64** (1990) 1377.

[5] SANTAMATO E., DAINO B., ROMAGNOLI M., SETTEMBRE M., SHEN Y. R., *Phys. Rev. Lett.* **61** (1988) 113.

[6] SANTAMATO E., ABBATE G., MADDALENA P., *Phys. Rev.* **A 38** (1988) 4323.

[7] Back-flow and inertial terms are neglected. Moreover, one viscous constant γ is used.

[8] Equation (4.9) of Ong's paper in [3]. See also ONG H. L., *Appl. Phys. Lett.* **46** (1985) 822. In terms of the material constants this condition reads $k_{11}/k_{33} + 9\, n_o^2/4\, n_e^2 < 9/4$.

[9] ONG H. L., SCHADT M., CHANG I. F., *Mol. Cryst. Liq. Cryst.* **132** (1986) 45.

[10] The actual angular velocity Ω of the precession is related to $\tilde{\Omega}$ by $\Omega = \left(\frac{k_{33}}{\gamma_1 L^2} \right) \tilde{\Omega}$ (rad/s).

[11] Preliminary observations of phase-locking and hysteresis in the OFT with linear polarization have been reported by ABBATE G., MADDALENA P., MARRUCCI L., SAETTA L. and SANTAMATO E., 3rd International Topical Meeting on « Optics of Liquid Crystals » (Cetraro, Italy, October 1-5) 1990.